BNL-211704-2019-TECH
CBETA/037

CBETA 4-pass orbit correction and tolerance study

W. Lou, S. Peggs

November 2018

Collider Accelerator Department
Brookhaven National Laboratory

U.S. Department of Energy
USDOE Office of Science (SC), Nuclear Physics (NP) (SC-26)

DISCLAIMER

CBETA Machine Note #037
CBETA 4-pass Orbit Correction and Tolerance Study*

W. Lou†
CLASSE, Cornell University, Ithaca, NY 14853, USA
(Dated: November 29, 2018)

I. INTRODUCTION

The main goal of this study is to find the tolerance of the CBETA FFAG lattice subjected to various errors. Common error sources include non-ideal magnet positioning and alignment, undesired multipole field strengths, and BPM offsets. In order to fix the beam trajectories (orbits) affected by the errors, dipole kickers have been allocated throughout the FFAG beamline to serve as correctors. Since there are four coexisting orbits in the FFAG, the correction scheme must aim to correct all four of them simultaneously. The simulation is performed using Bmad, developed by Cornell University to model relativistic beam dynamics in customized accelerator lattices [1]. The core of orbit correction is the singular value decomposition (SVD) optimization. As the error magnitudes increase, the beam size and emittance after correction could undesirably increase, and our goal is to find the "individual limit" of each error type beyond which the increases become unacceptable. Typically this limit is reached before the orbits become un-correctable. Similarly we can also find the "combined limit" of various errors. Both limits will be properly defined in the later section.

II. CBETA FFAG LATTICE

The CBETA FFAG beamline consists of 107 full cells and 2 half-cells (see Fig. 1). Each full cell consists of two quadrupole magnets, one BPM (orbit monitor), one horizontal and one vertical kicker. The two half-cells locate at the beginning and the end of the beamline, and are neglected in this study for simplicity. An important assumption in this study is that all the splitters are able to perfectly correct the orbit of each energy into the FFAG lattice. In other words the errors do not propagate from orbit to orbit over recirculation. However, all four orbits are still simultaneously affected by the errors and correctors.

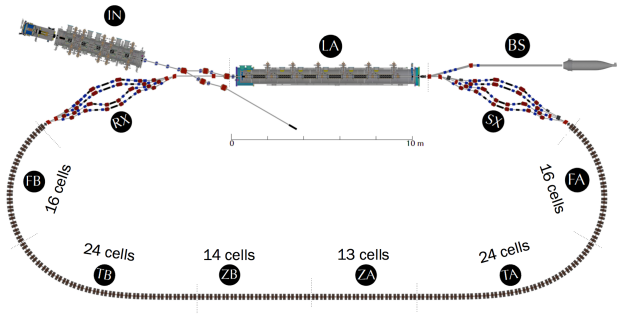

FIG. 1. Layout of CBETA. The sections labeled (IN) and (LA) are the injector and MLC cavities respectively. Sections (FA), (TA), (ZA), (ZB), (TB), and (FB) form the FFAG beamline which can accommodate four recirculating orbits with energy ranging from 42 MeV to 150 MeV. Sections (SX) and (RX) are splitters which control the path-length of each recirculation pass.

III. EXAMPLE SIMULATION

This section describes how Bmad corrects the FFAG orbits with a set of random b1 gradient error introduced to all the FFAG magnets. The details on how SVD optimization works will not be covered here. Fig. 2 shows the four design orbits in half of the FFAG beamline (FA, TA, and ZA). Note that the orbits are periodic in FA, and zero in ZA.

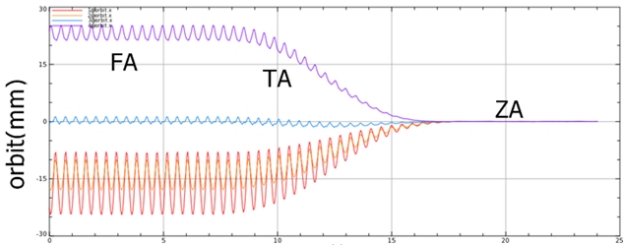

FIG. 2. The four design orbits in the first half of the FFAG beamline. The orbits in the other half is very close to the mirror image.

The top half of Fig. 3 shows the distorted orbits when all the FFAG quadrupole magnets incur a 0.5% Gaussian random error in their b1 gradient. Clearly the orbits become non-periodic in FA and non-zero in ZA. The bottom half of Fig.3 shows the recovered orbits after SVD orbit correction using all the horizontal kickers. Note that the orbit correction aims to recover the orbits only at the

* This work was performed with the support of NYSERDA (New York State Energy Research and Development Agency).
† wl528@cornell.edu

location of BPMs, the only places we can measure them in reality. For each cell we have 4 horizontal orbits to correct at the BPM, yet only one horizontal corrector to use (same for the vertical plane). Since the system is already over-constrained, requiring extra locations for corrected orbits could barely improve overall correction. However, it's possible to improve the correction by properly assigning weights to the correctors. This method involves further study in the SVD optimization, and is not invoked here.

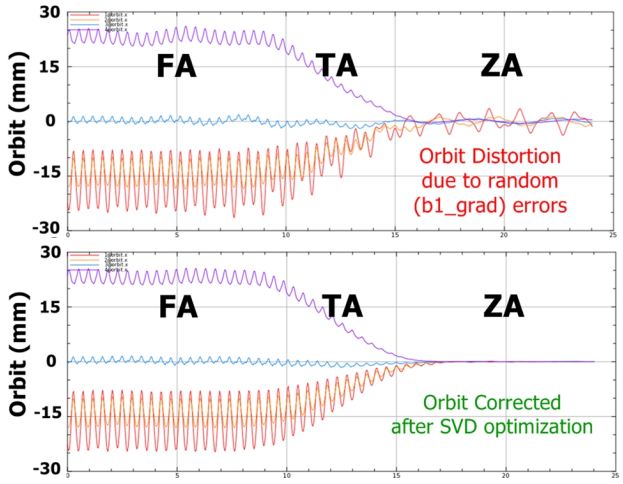

FIG. 3. The top half shows the orbit distortion with all FFAG quad magnets subjected to a 0.5% Gaussian random error in their b1 gradient. The bottom half shows the recovered orbits after SVD orbit correction.

IV. RESULT STATISTICS

For clarification, we call the correction process to a particular assignment of errors "one simulation". To determine the tolerance of the lattice subjected to certain error, we must run many simulations to obtain statistics. Fig. 4 illustrates the general procedure to determine the tolerance of an error, and Fig. 5 describes the procedure in details, including our definition of "individual limit".

For a chosen error type and error magnitude we run N=100 simulations to obtain a statistically representative "$\mu + 1\sigma$" (See Fig. 5). We call this quantity the "1σ increase" in X (or Y) emittance (or beam size). Fig. 6 shows that the 1σ increase in X emittance grows with error magnitude in b1 gradients. At 0.66% error in b1 gradients, the 1σ increase in X emittance reaches 10%. However, we also need to check the growth in the Y emittance and transverse beam sizes. Table 1 summarizes the required error magnitude for each 1σ increase to hit 10%. It turns out that the 1σ increase in Y beam size reaches 10% at 0.27% error in b1 gradient, earlier than the other three quantities. So the individual limit of b1 gradient error, by our definition, is 0.27%.

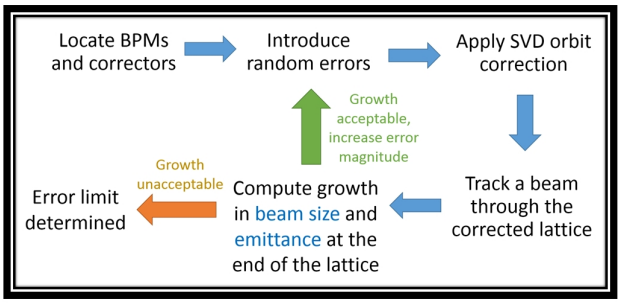

FIG. 4. A schematic diagram showing how the individual limit of a certain error is obtained using Bmad. The detailed description is in Fig.5.

(1) Choose a type of error(s)
(2) Choose a (reasonable) error magnitude
(3) Introduce random errors (Gaussian distribution) to the FFAG quads
(4) Decide which BPMs and correctors are to be used (usually all of them)
(5) Run the SVD optimizer to correct the orbit
(6) Track a beam through the lattice and record the X/Y emittance and beam_size at the end element (if no particle lost)
(7) Repeat (3) to (5) N times to calculate **"μ + 1σ"** in X/Y emittance/beam_size.
(μ + 1σ characterizes how bad emittance/beam_size could increase to)
(N>50 required for good statistics)
(8) Repeat (2) to (7) with different error magnitudes.
(9) Determine at which magnitude is any of the four "μ + 1σ" 10% greater than that of the no-error case. This is the **individual limit** of this error type.

FIG. 5. The detailed procedures to determine the individual limit of a certain error.

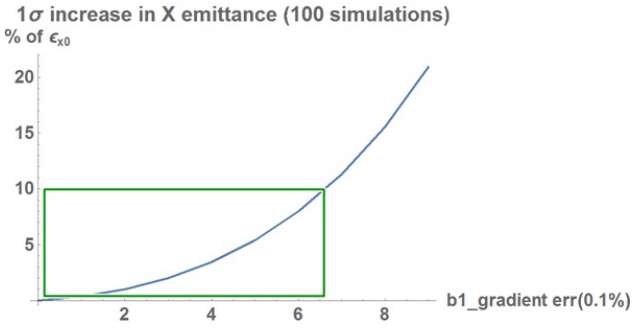

FIG. 6. The growth of 1σ increase in X emittance as the error magnitude in b1 gradient increases. The green rectangle shows that 10% increase is reached when b1 gradient magnitude hits 0.66%.

Quantity	Error magnitude in b1 gradient to hit 10% 1σ increase
X emittance	0.66%
Y emittance	0.90%
X beam size	0.37%
Y beam size	0.27%

TABLE I. The tolerance of FFAG beamline subjected to b1 gradient error.

V. INDIVIDUAL LIMITS OF VARIOUS ERROR TYPES

Similar to the b1 gradient error, 100 simulations were run to find out the individual limit of other error types. Table 2 shows the individual limits of a few common error sources. All these limits are above the design specification of CBETA, implying great tolerance of the design lattice.

Error Type		Individual limit
FFAG Magnets	Gradient	0.27%
	X offset	0.5 mm
	Y offset	> 0.5 mm
	tilt	6.5 mrad
BPM reading error		0.2 mm

TABLE II. The individual limit of common error types.

It's also important to find out the tolerance for higher order multipole fields, defined as:

$$B_x + iB_y = \frac{b_n + ia_n}{L}(x+iy)^n \tag{1}$$

,in which b_n and a_n are the strength for normal and skew multipole fields for $n \geq 2$. (b_1 is the normal quadrupole gradient, and b_2 is the normal sextuple moment.) L is the length of the magnet, and x and y are measured from the pipe center. For physically meaningful comparison, we normalize the multipole strengths in dimensionless unit u_0:

$$b_n = \left[10^{-4}\frac{GL}{r_0^{n-1}}\right]u_0 \tag{2}$$

, in which G is the quadrupole gradient, and r_0 is chosen to be 25 mm (about the extent of the highest and lowest energy orbit from the pipe center). Table 3 shows the individual limit of all the normal and skew multipoles, reported in u_0.

b2	37	a2	140
b3	30	a3	90
b4	26	a4	80
b5	21	a5	65
b6	21	a6	63
b7	19	a7	58
b8	21	a8	56
b9	18	a9	53

TABLE III. The individual limit of normal and multipole up to 20-pole, reported in the normalized unit u_0 .

VI. COMBINED LIMIT OF MULTIPOLE FIELD ERRORS

In reality all multiple sources of errors coexist, and the individual limits are insufficient to capture the whole picture. Instead, we need a statistically meaningful "combined limit". For now we consider just the 16 multipole field errors in table III. In the simulation we assign each FFAG magnet a 16-vector:

$$\mathbf{v} = \left(\frac{b_n}{lim\_b_n}, \frac{a_n}{lim\_a_n}\right), n = 2, 3...9 \tag{3}$$

in which lim_b_n and lim_a_n are the individual limits for proper weighting between the different multipoles. The value of each element in $\mathbf{v}$ is chosen randomly from the normal Gaussian distribution ($\mu = 0, \sigma = 1$). Since there are 16 errors present, the overall combined error must be first scaled down properly. A number u is chosen randomly from $(0, 1]$, and the 2-norm of the $\mathbf{v}$ (square root of sum of the squares) is scaled down to be $u^{(1/16)}$. This allows the $\mathbf{v}$ to point at a uniformly random point in the 16-D hyper-sphere of radius 1. We now further introduce a quantity "error scale" which scales all the elements in $\mathbf{v}$ by the same factor. By definition, the 2-norm also scales by the same factor, so we can use the 2-norm as a measure of the combined error.

Fig.7 shows the 1σ increase in X beam size grows with the error scale ranges from 0 to 1 at a step of 0.1. For each error scale 1000 simulations were run for representative statistics. At an error scale of 0.75, 1σ increase in X beam size reaches 10%, earlier than the other three quantities of interest. So the combined error for FFAG multipole field error is reported as:

$$\sqrt{\Sigma_n(\frac{b_n}{lim\_b_n})^2 + (\frac{a_n}{lim\_a_n})^2} < 0.75 \tag{4}$$

VII. FUTURE STUDIES

There are still many tolerance studies to be performed for the CBETA lattice. Perhaps the most important con-

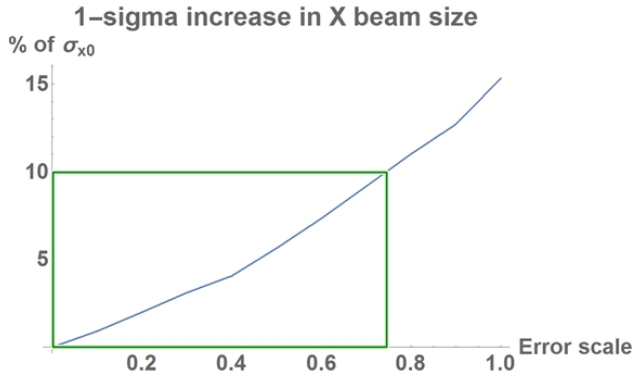

FIG. 7. The growth of 1σ increase in X beam size as the error magnitude in b1 gradient increases. The green rectangle shows that 10% increase is reached when b1 gradient magnitude hits 0.66%.

sideration is to use the entire 4-pass lattice with one design orbit, instead of only the FFAG beamline with 4 independent orbits. Although this would make optimization computationally more intense, it better simulates the reality. Similar to the having multipole field errors, we can also include different error sources together to investigate the overall combined tolerance.

[1] D. Sagan, *Bmad Simulation Software*, `https://www.classe.cornell.edu/bmad/`